THE UNIVERSITY of EDINBURGH

Edinburgh Research Explorer

Deposition of TS-1 zeolite film on palladium membrane for enhancement of membrane stability

Citation for published version:
Guo, Y, Wu, H, Jin, Y, Zhou, L, Chen, Q & Fan, X 2017, 'Deposition of TS-1 zeolite film on palladium membrane for enhancement of membrane stability', *International journal of hydrogen energy*, vol. 42, no. 44, pp. 27111-27121. https://doi.org/10.1016/j.ijhydene.2017.09.127

Digital Object Identifier (DOI):
10.1016/j.ijhydene.2017.09.127

Link:
Link to publication record in Edinburgh Research Explorer

Document Version:
Peer reviewed version

Published In:
International journal of hydrogen energy

General rights
Copyright for the publications made accessible via the Edinburgh Research Explorer is retained by the author(s) and / or other copyright owners and it is a condition of accessing these publications that users recognise and abide by the legal requirements associated with these rights.

Take down policy
The University of Edinburgh has made every reasonable effort to ensure that Edinburgh Research Explorer content complies with UK legislation. If you believe that the public display of this file breaches copyright please contact openaccess@ed.ac.uk providing details, and we will remove access to the work immediately and investigate your claim.

OPEN ACCESS

Download date: 12. Oct. 2024

Deposition of TS-1 zeolite film on palladium membrane for enhancement of membrane stability

Yu Guo[a,*] , Hongmei Wu[a,**], Yujia Jin[a], Lidai Zhou[a], Qiangqiang Chen[a], Xianfeng Fan[b]

[a]School of Chemical and Environmental Engineering, Liaoning University of Technology, Jinzhou 121001, PR China

[b]Institute for Materials and Processes, School of Engineering, The University of Edinburgh, King's Buildings, Mayfield Road, Edinburgh EH9 3JL, United Kingdom

Abstract

A thin TS-1 zeolite film was successfully fabricated on palladium membrane using an assembly method combined with secondary growth technique. The preparation of TS-1-Pd composite membrane involved three stages: (1) deposition of palladium layer on porous alumina support through electroless plating; (2) assembly of silicalite-1 zeolite seeds on the palladium layer; (3) growth of TS-1 layer from the zeolite seeds over the top surface of the palladium layer using hydrothermal synthesis method. The detailed microstructure of the TS-1-Pd composite membrane was examined by SEM, EDX, XRD, FT-IR and UV-vis. This architecture allows the composite membrane to remain stable for 10 days of hydrogen permeation tests at 773 K and tolerate 30 cycles in gas exchanging tests, even for 5 days of hydrogen permeation tests at 423 K. Furthermore, the presence of a TS-1 zeolite film on palladium membrane effectively

*Corresponding author. Tel.: +86 416 4199013; E-mail address: guoyulnut@163.com (Yu Guo)
**Corresponding author: Tel.: +86 416 4199013; E-mail address: wuhongmeilnut@126.com (Hongmei Wu)

protected the palladium membrane from the contamination from the hydrocarbon, therefore greatly enhanced its operation stability.

Keywords: Palladium membrane; Zeolite; Thin film; Hydrogen separation; Stability

1. Introduction

Hydrogen as a clean energy carrier has drawn much attention in the last decades [1-6]. For production of hydrogen, a variety of techniques have been developed, such as steam reforming of hydrocarbons, partial oxidation of fossil fuels, electrolysis of water, etc. However, hydrogen is not the only product from above mentioned methods. Therefore, obtaining highly pure hydrogen from the gas mixtures is the key point. Membrane technologies are expected to play a key role in separation and purification of hydrogen. Among various H_2-permeable membranes [7], palladium and palladium alloy membranes seems to be excellent candidates for applications in hydrogen separation and purification [8-14], fuel cells [15, 16], steam reforming [17-19] and H_2-related reactions [20-22] due to their excellent hydrogen permselectivity.

Based on the configuration, palladium-based membranes can be classified as two main types, palladium foil [23] and supported palladium membrane [24-31]. Compared to palladium foil, the supported palladium membrane has attracted intense interest owing to its low cost, excellent H_2 permeability and high physical strength. Despite extensive contributions which have been made on the preparation of supported palladium membranes, the membrane stability is still an obstacle for their applications in industries [32-35]. For instance, most studies focused on the preparation of

palladium-based membrane on the outer surface of porous support [36-40]. Under such way, the palladium membranes can be easily polluted and scratched during the operation, resulting in a decrease of their H_2 permeation performance and stability, even failure.

On the other hand, palladium membranes are often exploited for dehydrogenation process of hydrocarbons, such as dehydrogenation of propane to propylene [41] and dehydrogenation of ethylbenzene to styrene [42, 43]. By combining separation and catalytic functionalities in a single membrane reactor, instantaneous removal of hydrogen in the reaction zone by permeation through a membrane can increase the conversion. However, degradation of palladium membrane is often observed when they were applied to separate hydrogen from those carbon-containing gas mixtures. During the separation process of hydrogen, the palladium layer directly exposed to the feeding gas was prone to be contaminated and poisoned by carbon, resulting in a loss of hydrogen permeability [44, 45].

Recently, a novel strategy to enhance the stability of palladium membrane has been reported, in which a zeolite film as a protective layer was deposited on the surface of palladium membrane. This sandwich-like structure significantly improved the membrane stability. Abate et al.[46] reported that a TS-1 zeolite film was fabricated on the palladium membrane by secondary growth technique, including seeding of palladium membrane with TS-1 nanocrystals followed by hydrothermal synthesis. During the seeding process, polymers have to be used to increase the adhesion between TS-1 particles and the palladium membrane. Yu et al. [47] used the dilute acid to

pre-treat palladium membrane to form the imperfections of palladium membrane. This morphology will improve the adhesion of zeolite film on the palladium membrane. Evidently, fabricating a continuous and compact zeolite film on a palladium membrane is quite challenging, owing to their different chemical characteristics.

This paper presents a novel method to fabricate a TS-1 zeolite film on the palladium membrane using an assembly method combined with secondary growth technique to enhance the membrane stability. The microstructure and morphology of the TS-1-Pd composite membrane were characterized by SEM, EDX, XRD, FT-IR and UV-vis. The membrane stability was evaluated by long-term operation test, gas exchange cycling test. Moreover, the effect of propylene on hydrogen permeation properties of the TS-1-Pd composite membrane was also investigated.

2. Experimental

2.1 Materials

N_2H_4, Na_2EDTA, $SnCl_2$, HCl, NH_4OH, and TEOS, which were used for synthesis of palladium membrane and TS-1 zeolite film, were purchased from Tianjin Kermel Chemical Reagent Co. Ltd. The tetrapropyl ammonium hydroxide (TPAOH, 20 wt.%) was prepared in the laboratory. The $PdCl_2$ was provided by Shanghai Jiuling Chemical Co. Ltd. A porous alumina tube (O.D. 13 mm, I.D. 9 mm, length 75 mm, nominal pore diameter 200 nm) was provided by Foshan Ceramics Research Institute of China.

2.2 Fabrication of TS-1-Pd composite membrane

Fabrication of palladium membrane. The palladium membrane was fabricated on the porous alumina support by electroless plating. Prior to plating, the substrate was

activated by a $SnCl_2/PdCl_2$ method at room temperature. The activation process was composed of a two-step immersion sequence in an acidic $SnCl_2$ solution (2 g/L), followed by an acidic $PdCl_2$ solution (0.2 g/L). Then the palladium membrane was prepared by electroless plating at 318 K using the plating solution [48] containing $PdCl_2$ (3.5 g L^{-1}), Na_2EDTA(30 g L^{-1}), NH_4OH (15 M, 101 ml L^{-1}) and N_2H_4 (1 M, 16 ml L^{-1}).

Assembly of silicalite-1 (Sil-1) zeolite seeds on palladium membrane. The resulted palladium membrane was functionalized with 3-aminopropyltrimethoxysilane (APTMS). During this process, the palladium membrane was placed in APTMS solution of ethyl alcohol (1:40 v/v) in a sealed autoclave and was heated at 373 K for 4 h. The unreacted organic linkers were washed away from the surface palladium membrane with ethanol. Subsequently, the APTMS-treated palladium membrane was immersed in an autoclave containing 0.08 wt.% silicalite-1(Sil-1) zeolite suspension of ethanol for 4 h at 373 K to assemble the zeolite seeds on the membrane surface. The Sil-1 zeolite seeds were synthesized from a solution with molar composition of 25 TPAOH:100 TEOS:2700 H_2O at 368 K for 24 h as described by Zhang et al. [49].

Growth of TS-1 zeolite. After seeding palladium membrane, the TS-1 zeolite layer was grown on the top surface of the palladium membrane using hydrothermal synthesis from a synthesis solution with a molar composition of 1 TEOS: 0.01 TBOT:0.18 TPAOH: 250 H_2O [50, 51]. A seeded palladium membrane was immersed in the synthesis solution in a Teflon vessel, which was sealed in a stainless steel autoclave at 448 K for 72 h. Thereafter, the resulted TS-1-Pd composite membrane was rinsed with deionized water, dried overnight at 373 K and calcined for 6 h at 823 K in nitrogen

atmosphere to remove the organic template.

2.3 Characterization

The morphologies of silicalite-1(Sil-1) zeoite seeds, palladium membrane, the seeded palladium membrane with Sil-1 zeolites and the TS-1-Pd composite membrane were examined by field emission scanning electron microscopy (FESEM, Hitachi S-4800). The X-ray diffraction (XRD) analysis was carried out with a D/Max2400 Rigaku X-ray diffractometer using Cu Kα radiation at 40 kV and 50 mA. Elemental composition of the samples was measured by Energy dispersive X-ray spectroscopy (EDXS, Bruker-quantax). Fourier transform infrared spectra (FT-IR) was recorded on an EQUINOX55 spectrometer (Bruker) using the KBr disk technique. The resulted samples were also analyzed by JASCO V-550 diffuse reflectance UV-vis spectrometer with $BaSO_4$ as the internal standard.

2.4 Permeation test

Permeation test of TS-1-Pd composite membrane was carried out in a stainless steel reactor described in previous report [48]. The membrane was sealed in the permeation module using graphite O-rings. The permeation module was placed in a temperature-programmable furnace and heated to the desired temperatures with a heating rate of 1 K min^{-1}. A set of thermocouples (K-type) within the permeation module were used to monitor the temperature during the permeation test. The gases (hydrogen, nitrogen and propylene) were introduced to the permeation module by the mass-flow controller. The hydrogen permeance at the permeation side was measured at desired temperature using a soap-bubble flow meter.

To investigate the membrane stability, the TS-1-Pd composite membrane was tested for 10 days at 773 K. In addition, the membrane was subjected to rapid changes in hydrogen and nitrogen for 30 cycles at 773 K. Furthermore, the chemical stability of the resulting membrane was tested with the treatment of propylene (30 ml/min) for 30 min at 703 K, followed by the measurement of hydrogen permeance.

3. Results and discussion

3.1 TS-1-Pd composite membrane

The preparation of TS-1-Pd composite membrane is illustrated in Fig.1. The preparation procedure involves three stages: (1) deposition of palladium layer on porous alumina support through electroless plating; (2) assembly of silicalite-1 zeolite seeds on the palladium layer; (3) growth of TS-1 film on the top surface of the palladium layer using hydrothermal synthesis method.

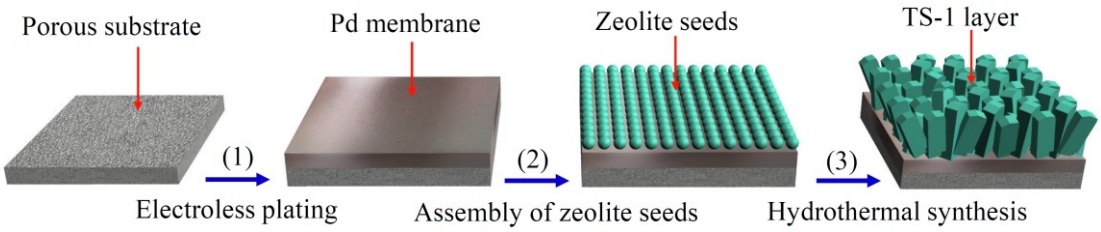

Fig.1 A schematic diagram of the preparation procedure for TS-1-Pd composite membrane.

For the preparation of palladium membrane on the non-conductive substrates including porous ceramic substrate or porous glass, electroless plating technique is one of the most effective methods in comparison with electroplating [52], chemical vapor deposition [53] and sputtering [23]. Fig.2a and b show that the non-conductive substrate

(porous alumina support) has smooth surface and nominal pore size of 200 nm. Fig.2c and d exhibit the SEM images of the palladium membrane prepared by electroless plating. A dense and smooth palladium layer was obtained on the alumina support (Fig.2c). No defects or cracks could be observed. As shown in Fig.2d, a palladium membrane with thickness of 6 μm was firmly connected to the substrate surface.

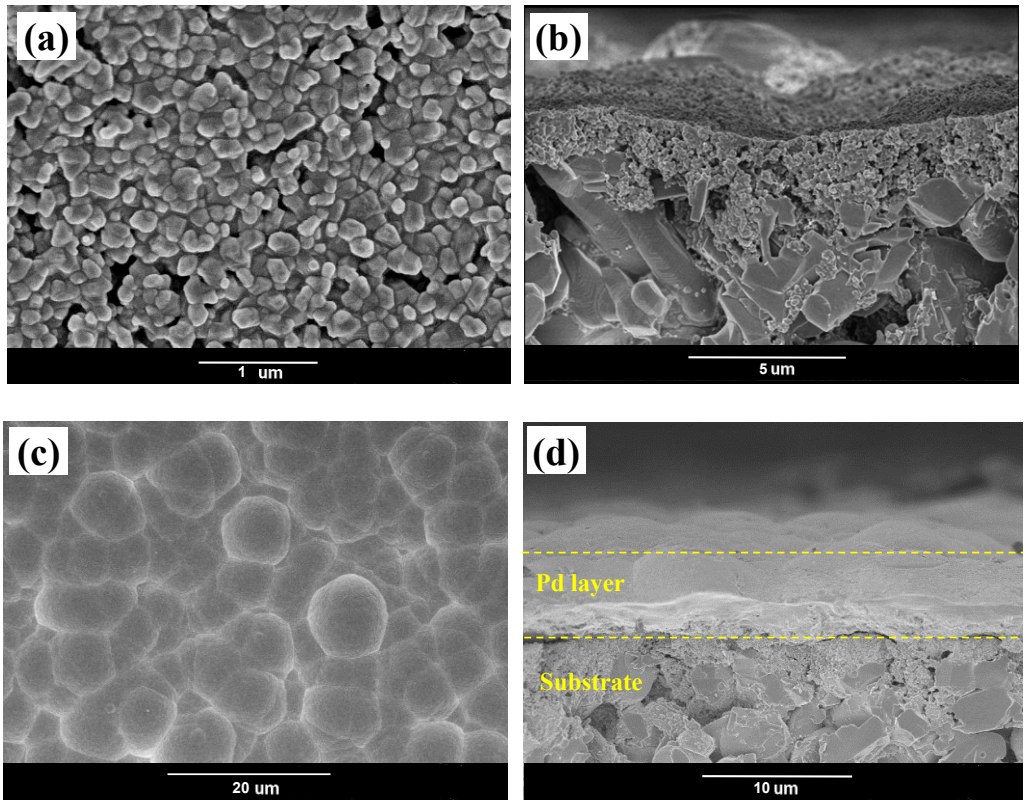

Fig.2 SEM images of porous substrate (a, b) and palladium membrane (c, d)

The secondary growth technique is a common method for the synthesis of zeolite films on substrates, involving deposition of zeolite seeds on a support followed by hydrothermal crystallization, due to its flexibility in controlling the orientation of the zeolite crystals and the microstructure of the zeolite film. A number of studies focused on the growth of zeolite film on different substrates, such as porous supports [50] and

non-porous metal substrates [54]. The seeding process of substrate plays a key role in the synthesis of the zeolite film by the secondary growth technique. The zeolite seeds will offer the crystal nuclei for the growth of zeolite film. In general, the zeolite seeds could be easily deposited on the porous substrate by dip-coating method mainly due to the capillary force. Nevertheless, this method is not very useful to deposit the zeolite seeds on the non-porous metal substrates, such as gold, copper and nickel. Therefore, pretreatments of the non-porous metal substrates are necessary. In our method, the surface of the resulted palladium membrane was pretreated with silane coupling agents (APTMS) to form a linker between the TS-1 zeolite and the palladium membrane.

Prior to depositing TS-1 zeolite film on the palladium membrane, Sil-1 zeolite seeds with particle size of 200~300 nm were prepared, as shown in Fig.3a. The Sil-1 zeolite seeds were then uniformly attached and assembled on the surface of the palladium membrane through APTMS linkers, as presented in Fig.3b. During the seeding process, the APTMS linkers can attach to palladium surface through the NH_2 groups, which is similar to that in the previous reports [55, 56]. The alkoxysilane group of the APTMS linkers tethered on the surface of palladium membrane will connect with the hydroxyl groups on the Sil-1 zeolite surface. These zeolite seeds will provide nuclei for further growth of TS-1 zeolite layer. In comparison, the palladium membrane was seeded without the assistance of APTMS. As presented in Fig.3c, only some Sil-1 zeolite particles scattered on the palladium membrane. This indicates that APTMS as a linker plays an important role in the seeding process of palladium membrane. The EDX analysis of the seeded palladium membrane shown in Fig.3d clearly indicates that

silicon (Si Kα) and palladium (Pd Lα$_1$) along with oxygen (O Kα) were detected. This result also confirmed that the Sil-1 zeolite seeds were dispersed on the surface of the palladium membrane.

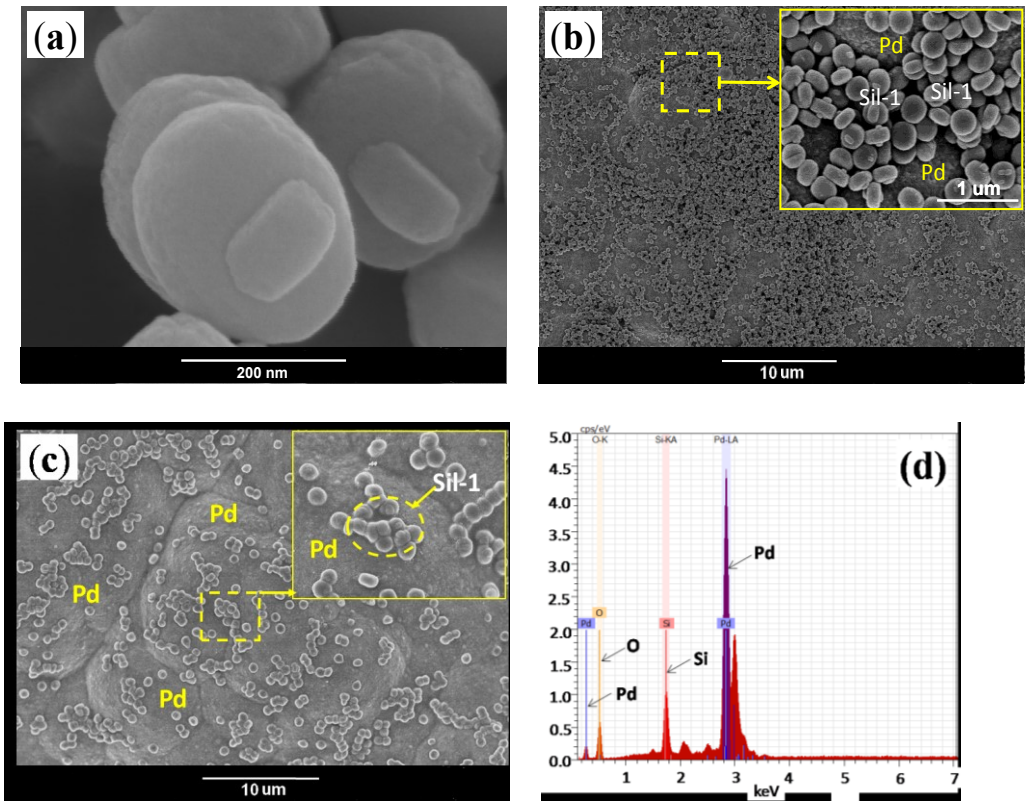

Fig. 3. SEM images of Sil-1 zeolite seeds (a), seeded palladium membrane with (b) and without (c) assistance of APTMS, respectively. EDX analysis of the seeded palladium membrane (d).

According to the dissolution-recrystallization growth mechanism for the synthesis of the zeolite by hydrothermal synthesis, the Sil-1 zeolite seeds on the palladium membrane will grow to a continuous TS-1 zeolite film. Fig. 4a presents the SEM image of the TS-1-Pd composite membrane. It reveals that the palladium membrane surface was fully covered with compact and well intergrown TS-1 zeolite crystals. No

palladium layer can be found. This indicates that the palladium layer will be protected very well by the zeolite layer. In contrast to the cross-sectional view of palladium membrane (Fig.2d), it can be clearly seen in Fig.4b that an additional TS-1 film with thickness of 2 μm was formed on the top surface of the palladium membrane. However, when the seeding process was carried out without the assistance of APTMS, obvious defects can be observed in the resulted TS-1 film, as displayed in Fig.4c. The palladium membrane was not fully covered by TS-1 zeolite crystals. This is attributed to the poor seeding of the palladium membrane, as shown in Fig.3c. In addition, compared to the secondary growth technique, TS-1 zeolite film was prepared on the palladium membrane using directly hydrothermal synthesis without seeding process. From the SEM image presented in Fig.4d, only some scattered TS-1 zeolites were deposited on the palladium membrane. It reveals that a continuous and dense TS-1 zeolite film could not be easily formed without zeolite seeds on the palladium membrane.

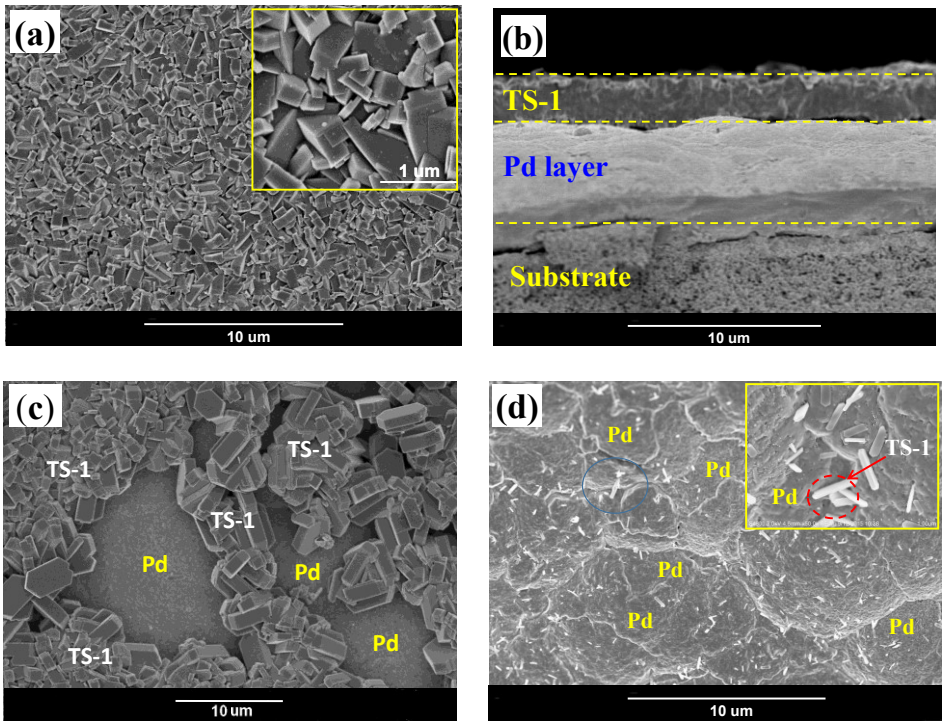

Fig.4. SEM images of TS-1-Pd composite membranes prepared by hydrothermal synthesis with (a, b) and without (c) assistance of APTMS and directly hydrothermal synthesis without seeding process (d), respectively.

To further understand the structure of the TS-1-Pd composite membrane, the elemental distribution of the composite membrane was studied by EDX lining analysis. As shown in Fig.5, the Pd signal between the TS-1 layer (Ti, Si and O signals) and the porous alumina support (Al signal) was clearly observed. This reveals that the TS-1-Pd composite membrane has sandwich-like structure, which is in good agreement with the SEM result displayed in Fig.2d.

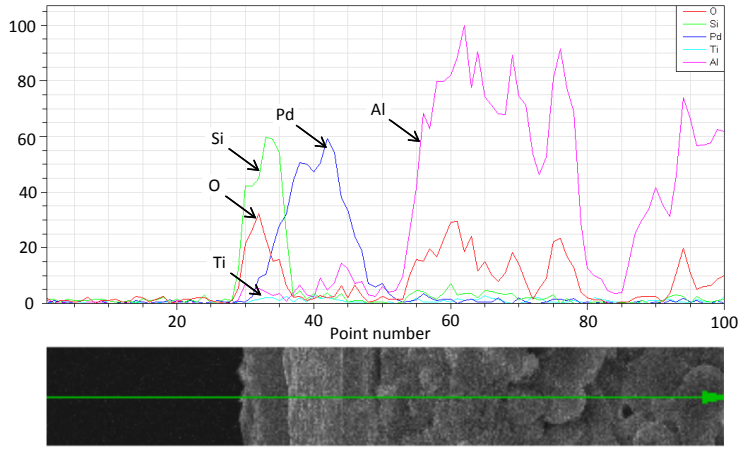

Fig.5. EDX lining analysis of the TS-1-Pd composite membrane.

The X-ray diffraction patterns have also confirmed the sandwich-like structure of the TS-1-Pd composite membrane, as shown in Fig.6a~6c. For the palladium membrane deposited on the porous alumina, only the characteristic peaks of pure palladium could be seen in Fig.6b, suggesting that the palladium layer is dense. After synthesizing TS-1 zeolite film, apart from typical palladium peaks, characteristic peaks of TS-1 zeolite

were also clearly observed in Fig.6c. This indicates that the TS-1 zeolite layer was successfully fabricated on the outer surface of palladium membrane. Moreover, no diffraction peak of alumina was detected on the TS-1-Pd composite membrane, suggesting the integrity of the palladium membrane was not affected during the formation of TS-1 zeolite layer by hydrothermal synthesis. Fig.6d shows FT-IR spectrum of the TS-1 zeolite powders collected at the bottom of synthesis autoclave. It indicates that absorption peaks at 1220 cm^{-1}, 1100 cm^{-1}, 800 cm^{-1}, 550 cm^{-1} and 450 cm^{-1} were clearly seen. These peaks were assigned to the characteristic bands of MFI zeolite [57]. Besides, the infrared signal at about 960 cm^{-1} is commonly originated from Ti-O-Si and often taken as the fingerprint of titanium substitution in the zeolite framework [58]. Moreover, Fig.6e presents the UV-vis spectrum of the TS-1 zeolite crystals. It can be found that the zeolite exhibits a dominant peak at 220-240 nm, which is assigned to the presence of the tetrahedral titanium in the zeolite framework. As expected, the characteristic adsorption peak of anatase TiO_2 at 330 nm was not observed, which confirms that the only tetrahedral coordinated titanium was formed in the zeolite framework [59].

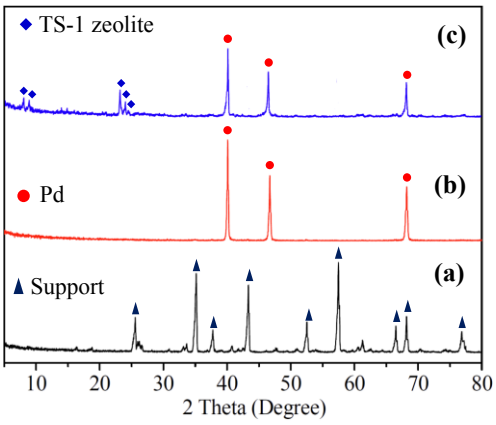

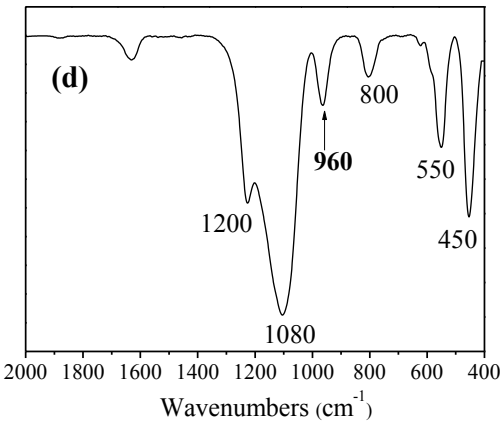

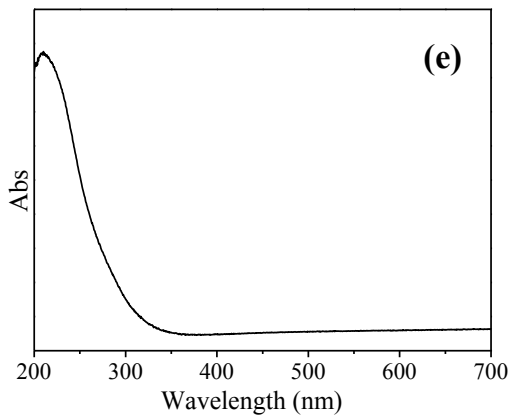

Fig. 6. The XRD patterns of alumina support (a), palladium membrane supported on alumina substrate (b) and TS-1-Pd composite membrane (c). FT-IR (d) and UV-vis (e) spectra of the TS-1 zeolite collected at the bottom of synthesis autoclave.

3.2 Hydrogen permeation performance

To investigate the effects of TS-1 zeolite film on the hydrogen transport properties and stability of the TS-1-Pd composite membrane, permeation tests were performed with H_2 and N_2 at temperature range of 423~773K. Fig.7 plots the H_2 permeation fluxes of palladium membrane before and after zeolite regrowth at various temperatures and pressure differences. The palladium membrane and resulted TS-1-Pd composite membrane have H_2 permeances of 2.05×10^{-6} and 0.54×10^{-6} mol m^{-2} s^{-1} Pa^{-1}, respectively. These permeance values are comparable to other hydrogen-permeable membranes (Table 1). After growth of TS-1 zeolite on the palladium membrane, an obvious decease of hydrogen permeance for TS-1-Pd composite membrane was observed. This is attributed to the higher transport resistance across the compact TS-1 zeolite film. Yu et al. [46] reported that the presence of an additional zeolite film on top of the palladium membrane markedly decreased its hydrogen permeance. In addition, Ti element was introduced to synthesize TS-1 zeolite film. Fernandez et al. [65] reported that Ti has

strong chemical interaction with palladium, resulting in the low hydrogen permeance of palladium membrane.

Table 1 Comparison of hydrogen permeation flux for various hydrogen-permeable membranes

Membrane	Temperature (K)	Pressure difference (kPa)	H_2 flux (mol m^{-2} s^{-1})	H_2/N_2 Selectivity	Ref.
Pd/ZrO_2/PSS	773 K	100	0.083	160	[60]
MCM-22/silica/Al_2O_3	473 K	100	0.007	50	[61]
silica	773 K	100	0.018	730	[62]
ZIF-90	473 K	100	0.021	17.5	[63]
Pd/NaA	723 K	50	0.079	608	[64]
Pd/YSZ	673	110	0.0734	320	[36]
Pd	773 K	100	0.205	886	This work
TS-1-Pd	773 K	100	0.054	268	This work

According to Sieverts' law, the hydrogen flux is proportional to the square root of hydrogen partial pressure (pressure exponent n=0.5) when bulk diffusion through palladium layer is the rate-controlling step. When the surface process is important, this exponent corresponds to n=1. Fig.7 shows that the hydrogen flux is linearly proportional to the pressure difference across the membrane at different temperatures, reflecting the n value=1. Factually, the pressure exponent often deviated from 0.5, as reported by many researchers [31, 37, 38, 46], the differences of n-values would be attributed to the differences in the preparation method, surface activity, membrane microstructure and mass transfer resistance for palladium composite membranes. It is believed that the existence of TS-1 film decreases the surface which may be reached by H_2, because part of the palladium membrane is shielded from the deposited zeolite

crystals. This causes the change of surface activity and mass transfer properties of the palladium membrane, resulting in the increase of n value. On the other hand, the H_2 permeation flux increases with temperature and activation energies of 15.4 and 13.7 kJ mol^{-1} were obtained for the palladium membrane and resulted TS-1-Pd composite membrane, respectively. These values are comparable to that reported in other publications [34, 46].

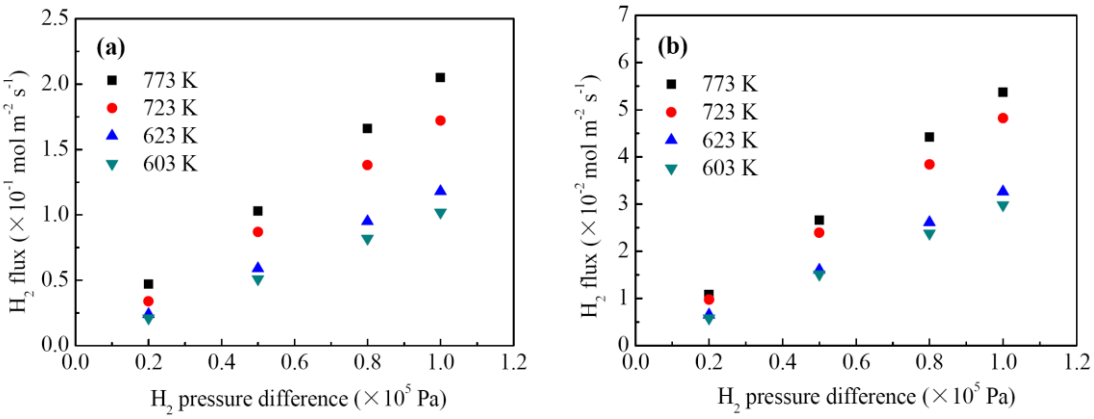

Fig. 7. The H_2 permeation fluxes of palladium membrane before (a) and after (b) zeolite regrowth at various temperatures and pressure differences.

Thermal and chemical stability of the palladium membranes remains as one of the major problems for their applications in industries. The formation of defects on palladium membranes has often been observed when undergoing thermal treatment for long-term operation and hydrogen absorption/desorption cycles [33]. To measure the stability of the TS-1-Pd composite membranes, long-term operation was carried out at 773 K and 423 K, as presented in Fig.8. The plots show that a stable hydrogen permeance was obtained during a continuous operation of 10 days at 773 K, even when the membrane was operated for 5 days of permeation at 423K which is below the

embrittlement temperature of palladium. In addition, the gas exchange cycle between hydrogen and nitrogen at 773 K and 100 kPa was also used to evaluate the stability of the resulting TS-1-Pd composite membrane. Fig.9 shows the hydrogen permeance almost kept unchanged after 30 cycles of the gas exchange between hydrogen and nitrogen. This indicates that the TS-1-Pd composite membrane has a good stability.

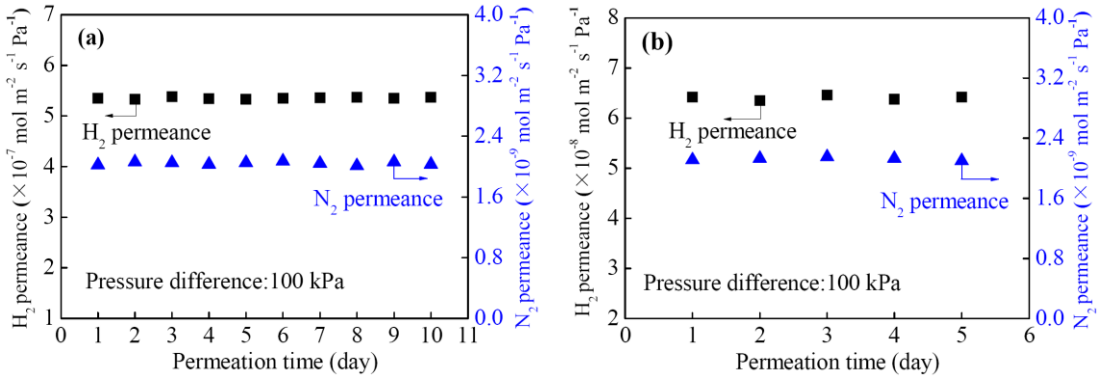

Fig.8. Long-term tests for the TS-1-Pd composite membrane at 773 K (a) and 423 K (b).

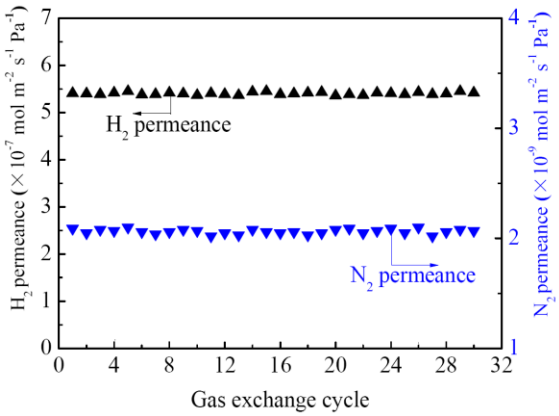

Fig.9. Gas permeances vs. gas exchange cycle between hydrogen and nitrogen at 773K for the TS-1-Pd composite membrane.

Furthermore, the effects of hydrocarbon on the hydrogen permeation performance of palladium composite membrane were investigated to determine the chemical stability of

the membrane. During the experimental process, propylene of 30 ml/min was introduced into permeate side of the membrane reactor for 30 min at 723 K. Then the gas flow was switched to the hydrogen from propylene, followed by measuring the hydrogen flux of the membrane. After the test, the hydrogen flux of the palladium membrane and TS-1-Pd composite membrane decreased 18% and 5% compared to the original hydrogen flux of the membranes, respectively, as shown in Fig.10. It revealed that propylene adsorption on the palladium membrane will affect the hydrogen permeability of the membrane. EDX analysis (not shown here) showed that a certain amount of carbon was observed on the membrane surface. This indicated that the palladium membrane was polluted by propylene, resulting in the decrease of the surface activity. Yu et al.[47] also found that some $Pd_{1-x}C_x$ phases formed on the palladium membrane after permeation test by propylene. However, the loss of hydrogen permeance for the TS-1-Pd composite membrane was much smaller than that for the pure palladium membrane. The results presented have demonstrated that the TS-1 zeolite layer as a protector was grown on the top surface of palladium membrane. This sandwich-like membrane configuration makes the TS-1-Pd composite membrane able to operate under harsh condition.

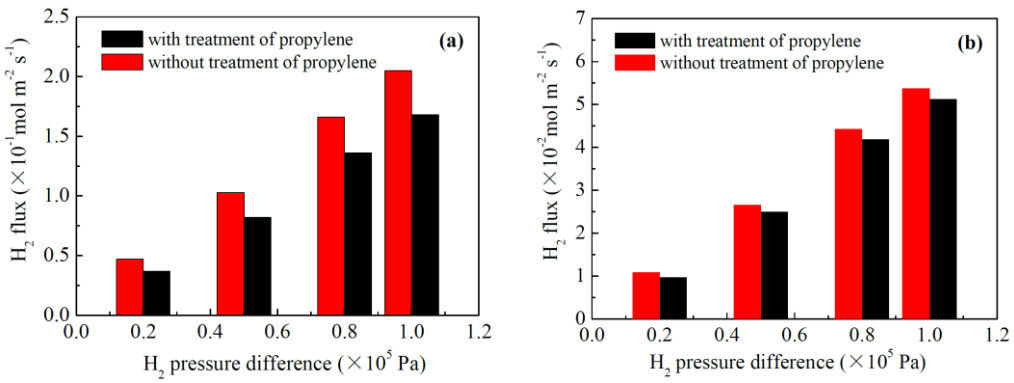

Fig.10. Effects of propylene on the hydrogen flux of pure palladium membrane (a) and TS-1-Pd composite membrane (b).

Reproducibility is a crucial factor for developing a novel fabrication method, which will influence the industrial mass production. A series of TS-1-Pd composite membranes were fabricated at the same synthesis condition. Table 2 lists the permeation test results of those TS-1-Pd composite membranes. The results show that all samples exhibited similar permeation selectivities and hydrogen fluxes at 773 K. In addition, the reproducibility was also evaluated by hydrogen permeation test at different temperatures and their distribution of data was shown in Fig. 11. The relative standard deviations in the H_2/N_2 selectivity were below 20%. The results of hydrogen permeation tests suggested that the reproducibility was acceptable for the fabrication method.

Table 2 The hydrogen permeation properties of the resulted TS-1-Pd composite membranes fabricated at same condition in permeation tests at 773 K.

Sample number	Temperature (K)	Pressure difference	H_2 flux (mol m^{-2} s^{-1})	H_2/N_2 Selectivity
1	773 K	100 kPa	5.41	268
2	773 K	100 kPa	5.92	244
3	773 K	100 kPa	4.98	205
4	773 K	100 kPa	5.15	221

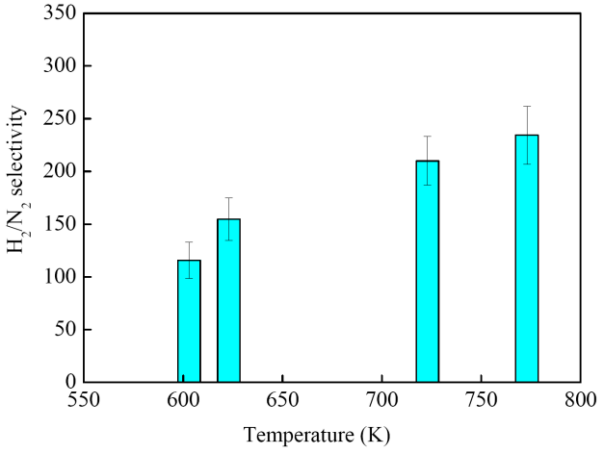

Fig.11. Reproducibility in fabrication of TS-1-Pd composite membranes that evaluated by hydrogen permeation tests at the temperature range of 603 K~773 K.

4. Conclusion

This work reports a novel method to fabricate a sandwich-like TS-1-Pd composite membrane to enhance the membrane stability. A continuous and compact TS-1 zeolite film was grown on the outer surface of palladium membrane using assembly method combined with secondary growth technique. The resulted TS-1-Pd composite membrane was stable for repeated cycling of gases and long-term operation at 773 K and 423 K. Furthermore, the existence of the TS-1 zeolite film can effectively suppressed the hydrogen flux loss from 18% to 5% reduction after pretreatment of the composite membrane in propylene atmosphere. In addition, the reproducibility in fabrication of TS-1-Pd composite membranes was acceptable, possessing a promising potential in the industry application.

Acknowledgments

This work was supported by the National Natural Science Foundation of China (21103076, 21601075), the Natural Science Foundation of Liaoning Province

(20170540435, 2015020249) and Program for Liaoning Excellent Talents in University (LJQ2012055).

REFERENCES

[1] Senseni AZ, Meshkani F, Rezaei M. Steam reforming of glycerol on mesoporous nanocrystalline Ni/Al_2O_3 catalysts for H_2 production. Int J Hydrogen Energy 2016; 41(44):20137–46.

[2] Allakhverdiev SI. Photosynthetic and biomimetic hydrogen production. Int J Hydrogen Energy 2012; 37(10): 8744–52.

[3] Meshkani F, Rezaei M. Hydrogen production by high temperature water gas shift reaction over highly active and stable chromium free Fe-Al-Ni catalysts. Int J Hydrogen Energy 2015; 40(34):10867–75.

[4] Ambrose AF, Al-Amin AQ, Rasiah R, Saidur R, Amin N. Prospects for introducing hydrogen fuel cell vehicles in Malaysia. International Journal of Hydrogen Energy 2017; 42(14):9125–34.

[5] Gallucci F, Basile A. Pd-Ag membrane reactor for steam reforming reactions: A comparison between different fuels. International Journal of Hydrogen Energy 2008; 33(6):1671–87.

[6] Meshkani F, Rezaei M. A highly active and stable chromium free iron based catalyst for H_2 purification in high temperature water gas shift reaction. International Journal of Hydrogen Energy 2014; 39(32):18302–11

[7] Gallucci F, Fernandez E, Corengia P, van Sint Annaland M. Recent advances on membranes and membrane reactors for hydrogen production. Chem Eng Sci 2013;

92:40–66.

[8] Peters TA, Kaleta T, Stange M, Bredesen R. Development of thin binary and ternary Pd-based alloy membranes for use in hydrogen production. J Membr Sci 2011; 383(1–2):124–34

[9] Yun S, Oyama ST. Correlations in palladium membranes for hydrogen separation: A review. J Membr Sci 2011; 375: 28–45.

[10] Brunetti A, Barbieri G, Drioli E. Upgrading of a syngas mixture for pure hydrogen production in a Pd-Ag membrane reactor. Chem Eng Sci 2009; 64(15): 3448–54.

[11] Fernandez E, Helmi A, Medrano JA, Coenen K, Arratibel A, Melendez J, de Nooijer NCA, Spallina V, Viviente JL, Zuñiga J, van Sint Annaland M, Pacheco Tanaka DA. Palladium based membranes and membrane reactors for hydrogen production and purification: An overview of research activities at Tecnalia and TU/e, Int J Hydrogen Energy 2017; 42(19):13763–76.

[12] Ryi SK, Park JS, Kim SH, Cho SH, Hwang KR, Kim DW. A new membrane module design with disc geometry for the separation of hydrogen using Pd alloy membranes. J Membr Sci 2007; 297: 217–25.

[13] Zhu B, Tang CH, Xu H., Su DS, Li H. Surface activation inspires high performance of ultra-thin Pd membrane for hydrogen separation. J Membr Sci 2017; 526:138–46.

[14] Zhang K, Way JD. Palladium-copper membranes for hydrogen separation. Sep Purif Tech 2017; 186:39–44.

[15] Vivanpatarakij S, Aiouache F, Assabumrungrat S. Performance of an improved

combination unit of Pd-membrane methane steam reformer and intermediate temperature solid oxide fuel cell (C-Pd-ITSOFC). Int J Hydrogen Energy 2015; 40(4): 1894–901.

[16] Swesi Y, Ronze D, Pitault I, Dittmeyer R, Heurtaux F. Purification process for chemical storage of hydrogen for fuel cell vehicles applications. Int J Hydrogen Energy 2007; 32(18): 5059–66.

[17] Basile A, Pinacci P, Iulianelli A, Broglia M, Drago F, Liguori S, Longo T, Calabrò V. Ethanol steam reforming reaction in a porous stainless steel supported palladium membrane reactor. Int J Hydrogen Energy 2011; 36(3):2029–37.

[18] Rei MH, Yeh GT, Tsai YH, Kao YL, Shiau LD. Catalysis-spillover-membrane. III: The effect of hydrogen spillover on the palladium membrane reactor in the steam reforming reactions. J Membr Sci 2011; 369(1-2): 299–307.

[19] Tosti S, Zerbo M, Basile A, Calabrò V, Borgognoni F, Santucci A. Pd-based membrane reactors for producing ultra pure hydrogen: Oxidative reforming of bio-ethanol. Int J Hydrogen Energy 2013; 38(1):701–7.

[20] Niwa S, Eswaramoorthy M, Nair J, Raj A, Itoh N, Shoji H, Namba T, Mizukami F. A one-step conversion of benzene to phenol with a palladium membrane. Science 2002; 295:105–7.

[21] Guo Y, Zhang XF, Zou HY, Liu HO, Wang JQ, Yeung KL. Pd-silicalite-1 composite membrane for direct hydroxylation of benzene. Chem Commun 2009; 39: 5898–900.

[22] Lundin STB, Law JO, Patki NS, Wolden CA, Way JD. Glass frit sealing method

for macroscopic defects in Pd-based composite membranes with application in catalytic membrane reactors. Sep Purif Tech 2017; 172:68–75.

[23] Tosti S, Bettinali L, Castelli S, Sarto F, Scaglione S, Violante V. Sputtered, electroless, and rolled palladium-ceramic membranes. J Membr Sci 2002; 196: 241–9.

[24] Guo Y, Wu HM, Zhou LD, Zhang ZB, Liu HO, Zhang XF. Fabrication of palladium membranes supported on a silicalite-1 zeolite-modified alumina tube for hydrogen separation. Chem Eng Tech 2014; 37:1778–86.

[25] Yeung KL, Christiansen SC, Varma A. Palladium composite membranes by electroless plating technique: Relationships between plating kinetics, film microstructure and membrane performance. J Membr Sci 1999; 159:107–22.

[26] Ayturk ME, Kazantzis NK, Ma YH. Modeling and performance assessment of Pd- and Pd/Au-based catalytic membrane reactors for hydrogen production. Energy Environ Sci 2009; 2:430–8.

[27] Zeng GF, Goldbach A, Xu HY. Impact of support mass flow resistance on low-temperature H_2 permeation characteristics of a $Pd_{95}Ag_5/Al_2O_3$ composite membrane. J Membr Sci 2009; 326(2):681–7.

[28] David E, Kopac J. Development of palladium/ceramic membranes for hydrogen separation. Int J Hydrogen Energy 2011; 36(7):4498–506.

[29] Hu X, Chen W, Huang Y. Fabrication of Pd/ceramic membranes for hydrogen separation based on low-cost macroporous ceramics with pencil coating. Int J Hydrogen Energy 2010; 35:7803–8.

[30] Chen WH, Tsai CW, Lin YL. Numerical studies of the influences of bypass on hydrogen separation in a multichannel Pd membrane system. Renewable Energy 2017; 104:259–70.

[31] Zhang XL, Xiong GX, Yang WS. A modified electroless plating technique for thin dense palladium composite membranes with enhanced stability. J Membr Sci 2008; 314: 226–37.

[32] Abu El Hawa HW, Lundin STB, Patki NS, Way JD, Steam methane reforming in a PdAu membrane reactor: Long-term assessment. Int J Hydrogen Energy 2016; 41(24):10193–201.

[33] Li H, Caravella A, Xu HY. Recent progress in Pd-based composite membranes. J Mater Chem A 2016; 4: 14069–94.

[34] Tong J H, Su LL, Haraya K, Suda H. Thin and defect-free Pd-based composite membrane without any interlayer and substrate penetration by a combined organic and inorganic process. Chem Commun 2006; 10: 1142–4.

[35] Zheng L, Li H, Xu HY. "Defect-free" interlayer with a smooth surface and controlled pore-mouth size for thin and thermally stable Pd composite membranes. Int J Hydrogen Energy 2016; 41: 1002–9.

[36] Huang Y, Dittmeyer R. Preparation of thin palladium membranes on a porous support with rough surface. J Membr Sci 2007; 302:160–70.

[37] Guo Y, Jin YJ, Wu HM, Zhou LD, Chen QQ, Zhang XF, Li XX. Preparation of palladium membrane on Pd/silicalite-1 zeolite particles modified macroporous alumina substrate for hydrogen separation. Int J Hydrogen Energy 2014; 39:

21044–52.

[38] Pan XL, Xiong GX, Sheng SS, Stroh N, Brunner H. Thin dense membranes supported on α-Al_2O_3 hollow fibers. Chem Commun 2001; 24:2536–7.

[39] Li XT, Li AW, Jim LC, Grace JR. Hydrogen permeation through Pd-based composite membranes: Effects of porous substrate, diffusion barrier and sweep gas. J Membr Sci 2016; 499:143–55.

[40] Melendez J, Fernandez E, Gallucci F, van Sint Annaland M, Tanaka DAP. Preparation and characterization of ceramic supported ultra-thin (~1μm) Pd-Ag membranes. J Membr Sci 2017; 528:12–23.

[41] Sheintuch M, Dessau RA. Observations, Modeling and Optimization of Yield, Selectivity and Activity during Dehydrogenation of Isobutane and Propane in a Pd membrane Reactor. Chem Eng Sci 1996; 51(4):535–47.

[42] She Y, Han J, Ma YH. Palladium membrane reactor for the dehydrogenation of ethylbenzene to styrene. Catal. Today 2001; 67:43–53.

[43] Hermann C, Quicker P, Dittmeyer R. Mathematical simulation of catalytic dehydrogenation of ethylbenzene to styrene in a composite palladium membrane reactor. J Membr Sci 1997; 136:161–72.

[44] Li H, Goldbach A, Li WZ, Xu HY. On CH_4 decomposition during separation from H_2 mixtures with thin Pd membranes. J Membr Sci 2008; 324(1–2): 95–101.

[45] Jung SH, Kusakabe K, Morooka S, Kim SD. Effects of co-existing hydrocarbons on hydrogen permeation through a palladium membrane. J Membr Sci 2000; 170(1): 53–60.

[46] Abate S, Díaz U, Prieto A, Gentiluomo S, Palomino M, Perathoner S, Corma A, Centi G. Influence of Zeolite Protective Overlayer on the Performances of Pd Thin Film Membrane on Tubular Asymmetric Alumina Supports. Ind Eng Chem Res 2016; 55:4948–59.

[47] Yu JF, Qi CC, Zhang JX, Bao C, Xu HY. Synthesis of a zeolite membrane as a protective layer on a metallic Pd composite membrane for hydrogen purification. J Mater Chem A 2015; 3:5000–6.

[48] Guo Y, Zhang XF, Deng H, Wang XB, Wang Y, Qiu JS, Wang JQ, Yeung KL. A novel approach for the preparation of highly stable Pd membrane on macroporous α-Al_2O_3 tube. J Membr Sci 2010; 362: 241–8.

[49] Zhang XF, Liu HO, Yeung KL. Influence of seed size on the formation and microstructure of zeolite silicalite-1 membranes by seeded growth. Mater. Chem. Phys. 2006; 96: 42–50.

[50] Guo Y, Jin YJ, Wu HM, Li DX, Fan XF, Zhou LD, Zhang XF. Direct synthesis of propylene oxide using hydrogen peroxide in a membrane reactor. Chem Pap 2017; 71:49–57.

[51] Wang XB, Zhang XF, Wang Y, Liu HO, Wang JQ, Qiu JS, Ho HL, Han W, Yeung KL. Preparation and performance of TS-1/SiO_2 egg-shell catalysts. Chem Eng J 2011; 175:408–16.

[52] Itoh N, Tomura N, Tsuji T, Hongo M. Deposition of palladium inside straight mesopores of anodic alumina tube and its hydrogen permeability. Micropor Mesopor Mater 2000; 39:103–11.

[53] Xomeritakis G, Lin YS. CVD synthesis and gas permeation properties of thin palladium/alumina membranes. AIChE J 1998; 44(1):174–83.

[54] Mintova S, Valtchev V, Konstantinov L. Adhesivity of Molecular Sieve Films on Metal Substrates. Zeolites 1996; 17 (5):462–65.

[55] Zhou JL, Zhang XF, Zhang J, Liu HO, Zhou L, Yeung KL. Preparation of alkali-resistant, Sil-1 encapsulated nickel catalysts for direct internal reforming-molten carbonate fuel cell. Catal Commun 2009;10:1804–7.

[56] Yang GH, Zhang XF, Liu SQ, Yeung KL, Wang JQ. A novel method for the assembly of nano-zeolite crystals on porous stainless steel microchannel and then zeolite film growth. J Phys Chem Solids 2007; 68(1):26–31.

[57] Au LTY, Mui WY, Lau PS, Ariso CT, Yeung KL. Engineering the shape of zeolite crystal grain in MFI membranes and their effects on the gas permeation properties. Micropor Mesopor Mater 2001; 47(2-3):203–16.

[58] Qiu FR, Wang XB, Zhang XF, Liu HO, Liu SQ, Yeung KL. Preparation and properties of TS-1 zeolite and film using Sil-1 nanoparticles as seeds. Chem. Eng. J. 147(2009) 316–22.

[59] Chen XS, Chen P, Kita H. Pervaporation through TS-1 membrane. Micropor Mesopor Mater 2008; 115:164–9.

[60] Wang D, Tong JH, Xu HY, Matsumura Y. Preparation of palladium membrane over porous stainless steel tube modified with zirconium oxide. Catal Today 2004; 93–95: 689–93.

[61] Choi J, Tsapatsis M, MCM-22/silica selective flake nanocomposite membranes for

hydrogen separations. J Am Chem Soc 2010; 132: 448–9.

[62] Tsuru T, Igi R, Kanezashi M, Yoshioka T, Fujisaki S, Iwamoto Y. Permeation properties of hydrogen and water vapor through porous silica membranes at high temperatures. AIChE J 2011; 57:618–29.

[63] Huang A, Caro J. Covalent Post-functionalization of zeolitic imidazolate framework ZIF-90 membrane for enhanced hydrogen selectivity. Angew Chem Int Ed 2011; 50 (21), 4979–82.

[64] Bosko ML, Ojeda F, Lombardo EA, Cornaglia LM. NaA zeolite as an effective diffusion barrier in composite Pd/PSS membranes. J Membr Sci 2009; 331:57–65.

[65] Fernandez E, Helmi A, Coenen K, Melendez J, Viviente JL, Tanaka DAP, van Sint Annaland M, Gallucci F. Development of thin PdeAg supported membranes for fluidized bed membrane reactors including WGS related gases. Int J Hydrogen Energy 2015; 40: 3506–19.